

# Topological Optimum Design of a Compliant Mechanism for Planar Optical Modulator

C. F. Lin<sup>1</sup> and C. J. Shih<sup>2</sup>

*Department of Mechanical and Electro-Mechanical Engineering  
Tamkang University  
Tamsui, Taiwan 251, R.O.C.  
E-mail: <sup>1</sup>890340036@s90.tku.edu.tw  
<sup>2</sup>cjs@mail.tku.edu.tw*

## Abstract

The rotator type of optical modulating component modulator requires a planar angular rotator to control different angles for modulating the dissimilar light. If simply using the S-shape beam to behave a pin-joint, the rotator angle will be limited. The design target accordingly needs to maximize the range of output angle for satisfying the prescribed linear output positions or can be a sort of the generation function between the input and output. This paper applies the material distribution method of SIMP (Solid Isotropic Microstructure with Penalization) in the topological optimization to deal it. The objective function consists of maximizing the output range and minimizing the error between prescribed function and real output function with volume limit as the design constraint. The model presented in this paper is a preliminary successful work that requires further efforts towards the practical phase.

**Key Words:** Topology Optimization, Compliant Mechanism, Structural Optimization, Micro-Electro Mechanical Structure, Engineering Design, Computer-Aided Design

## 1. Introduction

A compliant mechanism can be defined as that a structure utilizes its elastic characteristic to generate a specifying mobility on the predetermined portion. Different from the recognized rigid-linkage, the compliant mechanism has joint-like structure instead of the conventional joints to perform the relative motion of force and movement transmission. Such a flexure-generated mechanism can be broadly useful in engineering for overcoming the existing un-solving problems of stress concentration and structural fatigue. Particularly, in the current micro-age, the advantages of a compliant mechanism including the single formation, fewer assembly parts, manufacturing cost deduction and friction deduction between the contacts. Thus, the simple

compliant mechanism has been considerably applied to the structure of micro-electro mechanical system, such as the flexural beam and flexural diaphragm making the signal of the actuator due to the elastic deformation [1]. The method of pseudo-rigid body model [2] has been used to simplify the analysis and design to a simple compliant mechanism where the joint is simulated by a flexural rotating pivot. Such applications contain the micro-grip and the pantograph [3]. Another important method for the compliant mechanism design is topological optimization [4]. The earliest topology optimization had been used on the maximizing the structural stiffness. Later on, Bendsøe and Kikuchi [5] proposed homogenization theory method for fixing the design domain problems; however, this method is

not convenient for the complex structures or non-maximizing stiffness problems. Mlejenk et al. [6] and BendsØe et al. [7] further developed the material density method in which each normalized density of finite element is treated as a design variable. The Young's modules and the normalized density have the relation by multiply a penalty index. This method can improve the homogenization method and simplify the solution process, can be referred as power-law approach or SIMP (Solid Isotropic Microstructure with Penalization) method. The method of SIMP has been generally utilized to the research of compliant mechanisms [8].

Comb actuator and piezo-electrical actuator are popularly employed in micro electro-mechanical systems. Comb type can have contraction force without expansion force. However, piezo-type has the opposite effects. These two actuators can move linearly and no way to produce large displacement due to the fundamental acting principle. How to increase and enhance the usefulness in application range by constructing the compliant mechanism into the current actuators are necessary and challenge. Therefore, altering the actuating direction, amplifying the displacement and adjusting the output direction are valuable and interesting research topics.

The rotary type of optical modulating component modulator needs a planar angular rotator to control different angles and modulate the dissimilar light. When comb actuator pulls force to drag S-beam for simulating a pin-joint [9], the rotary angle is limited. The input voltage is proportional to the rotating angle of the planar rotator. The objective of this paper is to develop the design model for maximizing the range for the output rotator angle with a specifying small input force. The second objective is to build up an applicable model for satisfying the prescribed linear output motion, which can also be a prescribed function between input and output. For controlling the input force, the input driving force of a comb actuator can be written as [10]:

$$F = \frac{N\epsilon hV^2}{G} \quad (1)$$

where  $F$  represents the derived force,  $\epsilon$  represents the dielectric constant,  $h$  represents the height of the finger,  $V$  represents the applied voltage and  $N$  represents the number of fingers.

## 2. Analysis for the Compliant Amplifying Mechanism of a Planar Angular Rotator

The variable light can be obtained by adjusting the optical modulating component via the horizontal, vertical and rotational mechanical movement. A planar angular rotator is used for rotational movement by variable output angle. Figure 1 indicates the compliant mechanism [10] where A is the planar angular rotator, B is the compliant structure and C is the comb actuator. When the comb actuator pulls, through B's deformation, can yields to rotation of C. Four comb actuators also provide the equilibrium support. Figure 2 is the illustration for the rotation of the planar angular rotator through the deformation of four compliant structures. Figure 3 shows the detailed linkage motion of this mechanism in which the slider is pulled, S-shape structure provides the flexible, rotational effects and displacement to satisfy the geometrical requirements. The output to input ratio of the displacement is about 1:1, which means that there is no amplifying effect. However in MEMS, the rotating effect by S-shape compliant structure replacing pin-joint is sometime not enough. In other words, they need the certain amplification. Additionally, the proportional relation between input and output requires maintain correctly also is the probable objective for micro-machined optical modulating components.

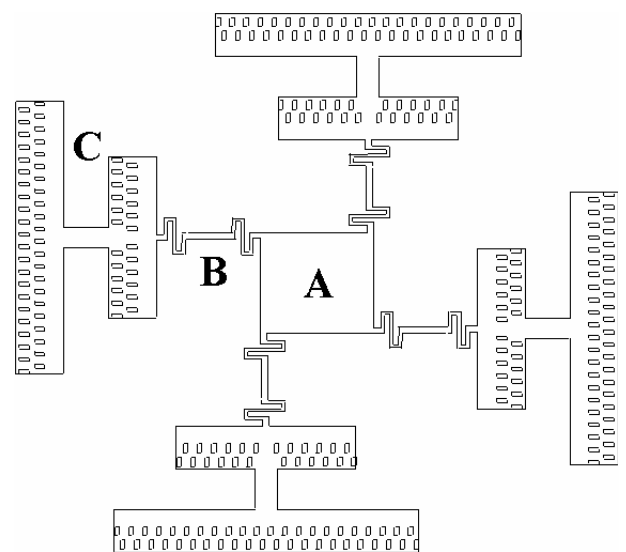


Figure 1. The compliant mechanism where A is the planar angular rotator.

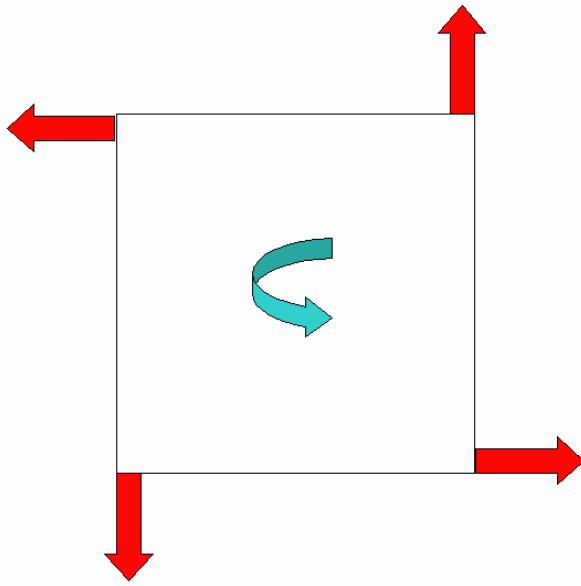


Figure 2. The illustration for the rotation of the planar angular rotator

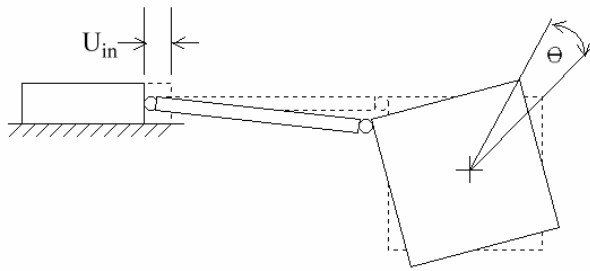


Figure 3. The linkage motion of the compliant mechanism

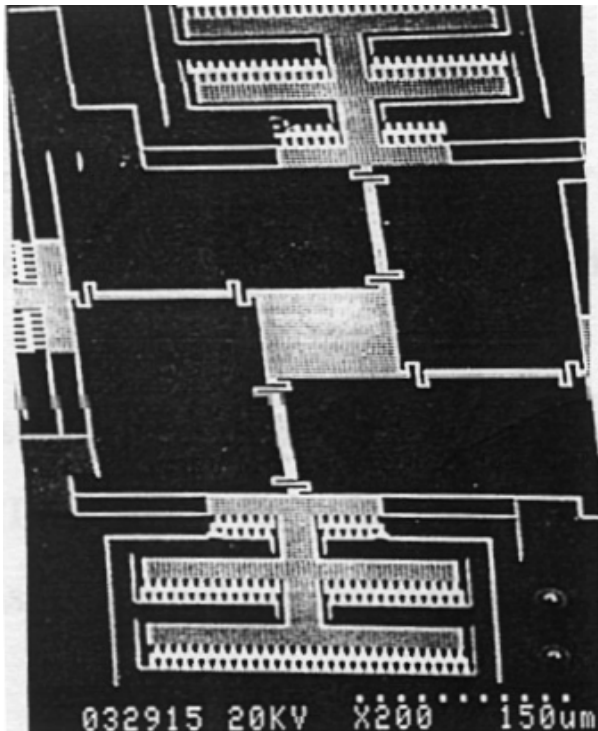


Figure 4. S-type planar compliant structure in Chen's work [10]

### 3. Topological Synthesis for an Amplifying Compliant Mechanism in Planar Angular Rotator

Figure 4 indicates the original structure in the Chen's work [10]. The planar angular rotator been driving and supports by these four compliant structures. In here, a quarter design domain indicating a single compliant mechanism was adopted as the design target. A linear spring was used to build and simplify the model for simulating the planar angular rotator. The input force is in the middle of left side for expressing the topological variation. The upper and lower corner has the supports in the design domain also for satisfying the boundary conditions in the finite element analysis. SIMP method is utilized in this study in which the normalized density  $\rho$  is setting as the design variable between 0 and 1. One also can think of it as the ratio of the material density to the original material density written as following:

$$x_i = \frac{\rho_i}{\rho_{i0}} \quad (2)$$

where  $\rho_{i0}$  is the  $i$ th original elemental density,  $\rho_i$  indicates the material density of the  $i$ th element. The value of  $\rho_i$  closing to zero means high removing possibility of the  $i$ th element. The Young's modulus of the  $i$ th element indicated as  $E_i$  that is assumed to have the relation with the original  $E_{i0}$  as:

$$E_i = x_i^\alpha E_{i0} \quad (3)$$

The value of  $\alpha$  is generally between 2 to 4 [11]. The larger  $\alpha$  represents the enhancing penalty effect so that the variation of  $E_i$  is serious.

The design model in this study is to maximize the output displacement, in other words, to obtain the maximum rotating angle of the planar device. The optimization formulation can be written as:

$$\text{Max } f(X) = U_{out,x}^2 + U_{out,y}^2 \quad (4)$$

$$\text{subject to } \sum_{i=1}^N x_i v_i \leq V \quad (5)$$

$$U_{in}(X) \leq C \quad (6)$$

$$0 \leq x_i \leq 1 \quad (7)$$

where  $x_i$  represent the  $i$ th normalized density variable,  $v_i$  represents the volume of each

element,  $U_{out,x}$  and  $U_{out,y}$  represents the output displacement corresponding to the x and y direction, respectively. The symbol  $U_{in}$  represents the input force displacement. The other design considerations include the prescribed linear motion of  $m$  points in the output motion. For obtaining this function generation problem, the topological optimization can be described as:

$$\text{Min } f(X) = \sum_{j=1}^M (U_{out,j} - U_{out,j}^*)^2 \quad (8)$$

subject to the same constructions of Equation (5) to (7). The  $U_{out,j}$  represents the output displacement due to the  $j$ th input and  $U_{out,j}^*$  represents the prescribed displacement. The sequential linear programming (SLP) has been applied to this study. The unit dummy load method [11] has been used for the sensitivity analysis of input and output. Sensitivity analysis of input displacement can be written as:

$$\{U\}^T \{F\}_{in} = U_{in} F_{in} = \{U\}^T [K] \{U\} \quad (9)$$

$$\frac{\partial U_{in}}{\partial x_i} F_{in} = \frac{\partial \{U\}^T}{\partial x_i} [K] \{U\} + \{U\}^T \frac{\partial ([K] \{U\})}{\partial x_i} = \frac{\partial \{U\}^T}{\partial x_i} [K] \{U\} \quad (10)$$

$$\text{where } \{F\}^T = \{U\}^T [K] \quad (11)$$

$$\frac{\partial \{F\}^T}{\partial x_i} = 0 = \frac{\partial \{U\}^T}{\partial x_i} [K] + \{U\}^T \frac{\partial [K]}{\partial x_i} \quad (12)$$

$$\frac{\partial \{U\}^T}{\partial x_i} = -\{U\}^T \frac{\partial [K]}{\partial x_i} [K]^{-1} \quad (13)$$

One can substitute (13) for (10) such that:

$$\frac{\partial U_{in}}{\partial x_i} = -\{U\}^T \frac{\partial [K]}{\partial x_i} \{U\} / F_{in} \quad (14)$$

By applying SIMP method to obtain the following:

$$[K] = \sum_{i=1}^n E_i [k_{i0}] = \sum_{i=1}^n x_i^\alpha E_{i0} [k_{i0}] \quad (15)$$

$$\frac{\partial [K]}{\partial x_i} = \frac{\alpha}{x_i} x_i^\alpha E_{i0} [k_{i0}] = \frac{\alpha}{x_i} [k_i] \quad (16)$$

Then it can be substituted into Eq. (14) to obtain the following:

$$\frac{\partial U_{in}}{\partial x_i} = -\frac{\alpha}{F_{in} x_i} \{u_i\}^T [k_i] \{u_i\} \quad (17)$$

For the first derivative of the specifying output point, one can assign a unit force  $F_d$  along the same direction so that:

$$\{U\}^T \{F\}_d = U_{out} F_d = \{U\}^T [K] \{U\}_d \quad (18)$$

$$\frac{\partial U_{out}}{\partial x_i} F_d = \frac{\partial \{U\}^T}{\partial x_i} [K] \{U\}_d + \{U\}^T \frac{\partial ([K] \{U\}_d)}{\partial x_i} \quad (19)$$

$$\frac{\partial U_{out}}{\partial x_i} = -\{U\}^T \frac{\partial [K]}{\partial x_i} \{U\}_d / F_d = -\frac{\alpha}{F_d x_i} \{u_i\}^T [k_i] \{u_i\}_d \quad (20)$$

The sensitivity of the output can be obtained by the chain rule as:

$$\frac{\partial U_{out}^2}{\partial x_i} = \frac{\partial U_{out}^2}{\partial U_{out}} \frac{\partial U_{out}}{\partial x_i} = 2U_{out} \frac{-\alpha}{F_d x_i} \{u_i\}^T [k_i] \{u_i\}_d \quad (21)$$

## 4. Design Example

### Case 1: Maximizing the Output Displacement or Output Angle

S-type planar compliant structure in [10] is the design simulation here, as shown in Figure 4. The design domain  $\Omega$ , its related geometrical dimensions and boundary are indicated in Figure 5. Input position has x motion only about  $\pm 10 \mu\text{m}$ . Left hand upper and lower corners are fixed with  $\pm 10 \mu\text{m}$ . Input static force is  $1000 \mu\text{N}$ . The Young's modulus is  $130 \times 10^3 \text{ N}/\mu\text{m}^2$ . The poison's ratio to 30 % of the original volume. The simulated spring constant is  $130 \times 10^3 \text{ N}/\mu\text{m}^2$ . There are total 2500 elements (or design variables) are used for optimize the equations 4 to 8. The total volume of the material is limited in 0.3, the prescribed input displacement is  $2.5 \mu\text{m}$ . Figure 6 is the final result of topological structure in which the output displacement is  $18.46 \mu\text{m}$ . The amplify effect is 7.32 with the max rotating angle  $14.62^\circ$ . When the final design model is given back to the completed structure, Figure 7 shows the complete geometrical configuration of the planar angular mechanism, and Figure 8 shows the motion of the complete mechanism. Using the finite element analysis when the final design model is given back to the completed structure, the structural performances are also shown in Table 1. One can

see the displacement and amplification are reduced on the completed structural performance. This phenomenon is reasonable because input work is equivalent to the elastic work of the compliant

mechanism plus the output work that results in the planar disk store some energy. However, the amplifying factor of 5.64 still is much larger than the original one.

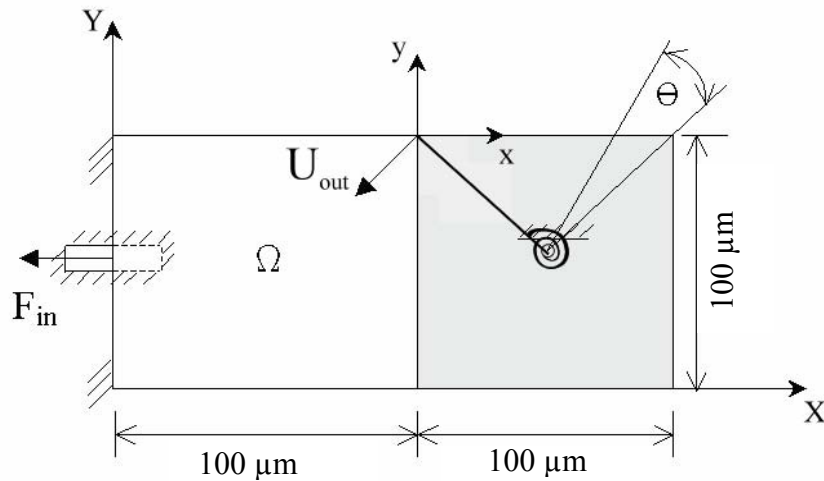


Figure 5. The design domain  $\Omega$  and related geometrical dimensions and boundary



Figure 6. The final result of topological design structure in Case 1

**Case 2: Linear Function Generation Mechanism**

All the conditions are the same as in the case 1 except the input load are 250, 500, 750 and 1000  $\mu N$  corresponding to the rotational angle  $\theta$  of  $3^\circ$ ,  $6^\circ$ ,  $9^\circ$  and  $12^\circ$ . The prescribed location can be prescribed as  $\{-4.3, 1.12\} \mu m$ ,  $\{-6.78, -4.03\} \mu m$ ,  $\{-9.11, -7.06\} \mu m$  and  $\{-11.28, -10.21\} \mu m$ . Figure 9 is the final result of topological structure in this design case. When the final design model is given back to the completed structure, Figure 10 shows the complete geometrical configuration of the planar angular mechanism, and Figure 11 shows the motion of the complete mechanism. Table 2 shows the performances of case 2 where indicate the model design and the complete structural design. Figure 12 shows the plot of the input and output performances in which the small circles indicate the prescribed response; however, the final topological design is marked with  $\times$ . Although the values are not precise enough, they still keep the linear relationship. Similarly, this model design is returned back to the completed structural arrangement, the final design is also in Table 2. It is not surprised to see the similar effects between Case 1 and Case 2.

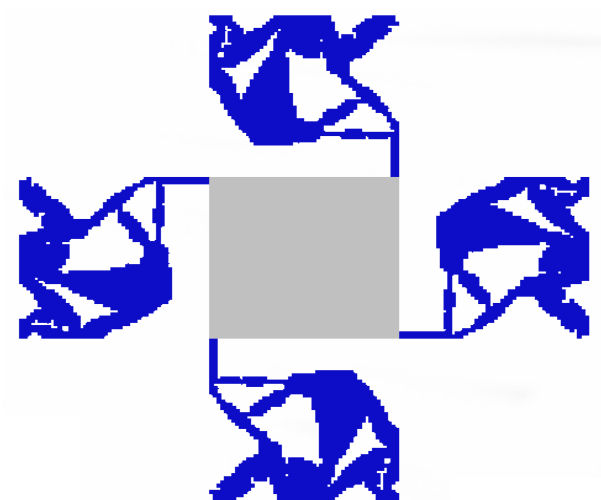


Figure 7. The complete geometrical configuration of the planar mechanism in Case 1



Figure 9. The final result of topological design structure in Case 2

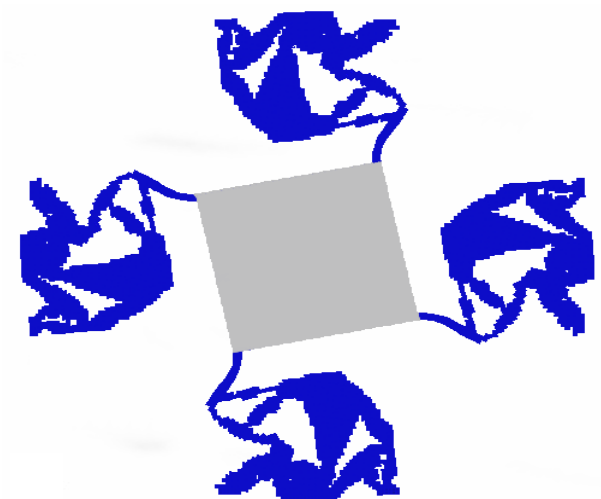


Figure 8. The motion of the complete mechanism in Case 1

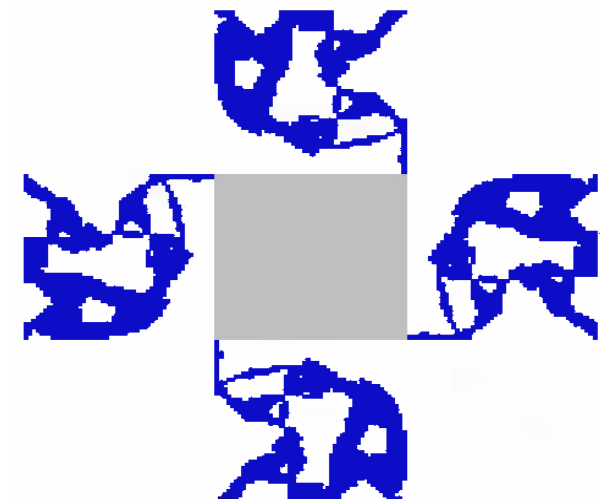


Figure 10. The complete geometrical configuration of the planar mechanism in Case 2

Table 1. The performances of the design Case 1

	Model design	Completed structural design
Input:	-2.52 $\mu\text{m}$	-1.039 $\mu\text{m}$
Output x,y:	(-13.05, -13.05) $\mu\text{m}$	(-4.143, -4.143) $\mu\text{m}$
Output movement:	18.455 $\mu\text{m}$	5.864 $\mu\text{m}$
Amplification:	7.32	5.64
Rotating angle:	14.62°	4.73°

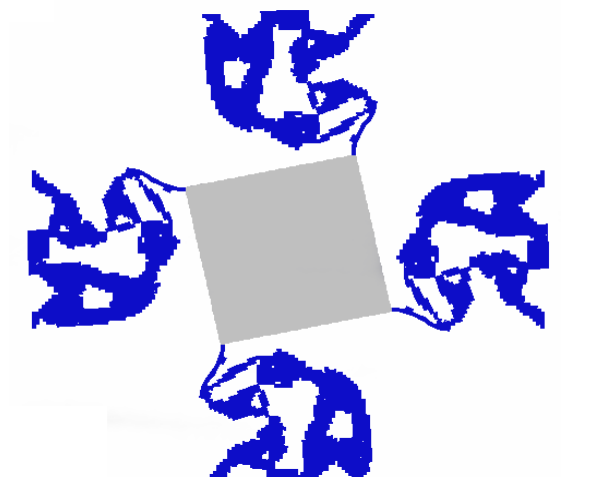


Figure 11. The motion of the complete mechanism in Case 2

Table 2. The performances of the design Case 2

	Model design	Completed
Load: 250 $\mu$ N		
Input:	-0.6638 $\mu$ m	-0.2897 $\mu$ m
Output x,y:	(-3.254,-3.252) $\mu$ m	(-1.120,-1.048) $\mu$ m
Output movement:	4.6011 $\mu$ m	1.5339 $\mu$ m
Rotating angle:	3.72°	1.24°
Load: 500 $\mu$ N		
Input:	-1.3276 $\mu$ m	-0.5794 $\mu$ m
Output x, y:	(-6.510,-6.504) $\mu$ m	(-2.239,-2.095) $\mu$ m
Output movement:	9.2023 $\mu$ m	3.0663 $\mu$ m
Rotating angle:	7.414°	2.478°
Load: 750 $\mu$ N		
Input:	-1.9915 $\mu$ m	-0.8691 $\mu$ m
Output x, y:	(-9.765,-9.756) $\mu$ m	(-3.359,-3.144) $\mu$ m
Output movement:	13.8034 $\mu$ m	4.6008 $\mu$ m
Rotating angle:	11.0449°	3.712°
Load: 1000 $\mu$ N		
Input:	-2.655 $\mu$ m	-1.159 $\mu$ m
Output x, y:	(-13.02,-13.008) $\mu$ m	(-4.478,-4.179) $\mu$ m
Output movement:	18.4046 $\mu$ m	6.1251 $\mu$ m
Rotating angle:	14.5876°	4.93°

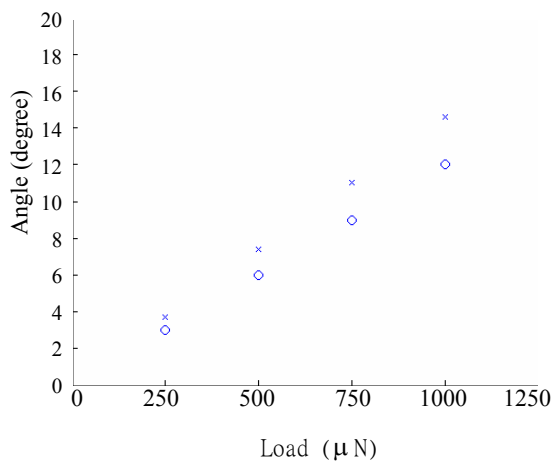


Figure 12. The plot of the input and output performances in Case 2

### 5. Conclusions

A preliminary design model presenting in this paper can be broadly accepted for simulating the pin-joint compliant mechanism in the rotating optical modulator because of the good amplifying

effects. The fractional designs show the further efforts are needed for improving the real necessity in the completed structure. The obvious amplifying and linear effects of the final design is encouragement to the future research, as compared to initial design. The practical topology structure of the presenting compliant mechanism requires additional modification for easily fabrication, also as the continuous research work.

### Acknowledgment

The support received from the National Science Council, Taiwan under Grant No. NSC 91-2212-E-032-004, is gratefully acknowledged.

### References

- [1] Fatikow, S. and Rembold, U., *Microsystem Technology and Microrobotics*, Springer-Verlag (1997).
- [2] Nielson, A. J. and Howell, L., "An Investigation of Compliant Micro-half-plates Using the Pseudo-rigid Body Model," *Mech. Struc. & Mach.*, Vol. 29, pp. 317-330 (2001).
- [3] Thomell, G., Bexell, M., Schweitz, J-A and Johansson, S., "The Design and Fabrication of a Gripping Tool for Micromanipulation," *The 8th International Conference on Solid-State Sensors and Actuators*, Sweden, Vol. 2, pp. 388-391 (1995).
- [4] Hetrick, J. A. and Kota, S., "An Energy Formulation for Parametric Size and Shape Optimization of Compliant Mechanisms," *Journal of Mechanical Design*, Vol. 121, pp. 229-234 (1999).
- [5] Bendsøe, M. P., and Kikuchi, N., "Generating Optimal Topologies in Structural Design Using a Homogenization Method," *Computer Method in Applied Mechanics and Engineering*, Vol. 71, pp. 197-224 (1988).
- [6] Mlejnek, H. P. and Schirmacher, R., "An Engineering's Approach to Optimal Material Distribution and Shape Finding," *Computer Method in Applied Mechanics and Engineering*, Vol. 106, pp. 1-26 (1993).
- [7] Bendsøe, M. P., and Haber, R. B., "The Michell Layout Problem as a Low Volume Fraction Limit of the Perforated Plate Topology Optimization Problem: an Asymptotic Study," *Structural Optimization*, Vol. 6, pp. 263-267 (1993).
- [8] Rozvany, G. I. N., "Aims, Scope, Methods, History and Unifed Terminology of

- Computer-aided Topology Optimization in Structural Mechanics,” *Struct. Multidisc. Optim.* Vol. 21, pp. 90-108 (2001).
- [9] Park, K. Y., Lee, C. W., Oh, S. Y. and Cho, Y. H., “Laterally Oscillated Forced-balanced Micro Vibratory Rate Gyroscope Supported by Fish Hook Shape Springs,” *MEMS '97, Proceedings, IEEE., Tenth Annual International Workshop*, pp. 494-499 (1997).
- [10] Chen, H., “The Study on The Micro-machine Optical Modulating Components,” Master’s Thesis, National Taiwan University, Taiwan, R.O.C. (1999).
- [11] Sigmund, O., "On the Design of Compliant Mechanisms Using Topology Optimization," *Mech. Struc. and Mach*, Vol. 21, pp. 493-524 (1997).

***Manuscript Received: Jul. 5, 2002  
and Accepted: Aug. 12, 2002***